



# Immobilization of 1,5,7-triazabicyclo [4.4.0] dec-5-ene over mesoporous materials: An efficient catalyst for Michael-addition reactions under solvent-free condition

Pranjal Kalita<sup>a,\*</sup>, Rajiv Kumar<sup>b</sup>

<sup>a</sup> Iowa State University, Department of Chemistry, Ames, Iowa 50011, USA

<sup>b</sup> Innovation Center, TATA Chemicals Ltd., Ghotavde Phata, Urawde Road, Pirangut Industrial Area, Gat No 1139/1, Mulshi, Pune 412108, India

## ARTICLE INFO

### Article history:

Received 13 November 2010  
Received in revised form 2 March 2011  
Accepted 5 March 2011  
Available online 12 March 2011

### Keywords:

Mesoporous materials  
1,5,7-triazabicyclo [4.4.0] dec-5-ene  
Michael-addition  
 $\beta$ -nitro styrene and malonate

## ABSTRACT

Immobilization of 1,5,7-triazabicyclo [4.4.0] dec-5-ene (TBD, a bicyclic guanidine base) over mesoporous material like SBA-15 has been found to be an excellent catalyst for Michael-addition of  $\beta$ -nitro styrene with malonate. The reactions were performed under solvent-free condition at 373 K for 9 h. A wide variety of Michael donors and acceptors were investigated. Among them, high yield of Michael product was obtained for the reaction between p-Cl-nitrostyrene with dimethyl malonate.

© 2011 Elsevier B.V. All rights reserved.

## 1. Introduction

There are many organic superbases [1] such as 1,5,7-triazabicyclo [4.4.0] dec-5-ene (TBD), 3,4,6,7,8-hexahydro-1-methyl-2H-pyrimido [1,2-a] pyrimidine (MTBD), 1,4-diazabicyclo [2,2,2] octane (DABCO), 1,8-diazabicyclo [5.4.0] undec-7-ene (DBU) and tetramethylguanidine (TMG), etc. Among the various organic superbases, 1,5,7-triazabicyclo [4.4.0] dec-5-ene (TBD) has been widely utilized in organic synthesis because of its high pKa value [2]. For example, TBD promotes various organic reactions such as Wittig reaction [3], nitroaldol (Henry) reaction [4], dialkyl phosphate addition to carbonyl compounds [4] and the addition of azoles to  $\alpha$ ,  $\beta$ -unsaturated nitriles and esters [5], and Baylis–Hillman reactions [6].

Several authors have reported Michael-addition of  $\beta$ -nitrostyrene to malonates [7], 1,3-dicarbonyl compounds [8], ketones [9], aldehydes [10], N-heterocycles [11] and indoles [12], using homogeneous catalyst. Very recently, Sartori reported [13] the similar type of reaction using silica supported organic bases including TBD under continuous-flow system condition. The

Michael-addition to nitroalkenes has been developed as a powerful tool in organic synthesis, because Michael adducts are versatile building blocks for agricultural and pharmaceutical compounds. For example, the Michael-addition of  $\beta$ -nitrostyrene to diethyl malonate produced Michael adducts.

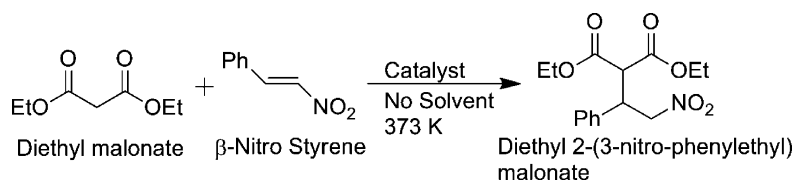
The immobilization of 1,5,7-triazabicyclo [4.4.0] dec-5-ene (TBD) in MCM-41 was first reported by Jacobs and co-workers and then catalyst was examined for Michael-addition of  $\alpha$ ,  $\beta$ -unsaturated ketone with malonate and Knoevenagel condensation [14]. Recently, immobilization of 1,5,7-triazabicyclo [4.4.0] dec-5-ene (TBD) in SBA-15 was reported by reported by Srivastava and then catalytic activity was examined for Mukaiyama-aldol and Michael reaction [15].

This paper deals with an effort towards developing green protocol for synthesis of diethyl 2-(3-nitro-phenylethyl) malonate and its derivatives by Michael-addition of  $\beta$ -nitrostyrene (nitro-alkene) and malonate using TBD immobilized mesoporous MCM-41/SBA-15 catalysts. The use of single step solventless conditions in combination with heterogeneous catalysts represents one of the main aspects of green chemical methods. For catalytic model reaction,  $\beta$ -nitrostyrene and diethyl malonate was chosen as starting material as shown in reaction Scheme 1. The effect of different mesoporous materials as support, effect of amount of catalyst, effect of temperature, recyclability of the catalyst and different substrates have been studied in this paper. A wide variety of Michael donors and acceptors were investigated. Among them, high yield of Michael product was obtained for the reaction between p-Cl-

\* Corresponding author.

E-mail addresses: [pkalita@iastate.edu](mailto:pkalita@iastate.edu) (P. Kalita), [rajiv.kumar@tatachemicals.com](mailto:rajiv.kumar@tatachemicals.com) (R. Kumar).

<sup>1</sup> Work carried out at Catalysis Division, National Chemical Laboratory, Pune 411008, India.



**Scheme 1.** Michael-addition of  $\beta$ -nitrostyrene and diethyl malonate.

nitrostyrene with dimethyl malonate. The product was successfully isolated by column chromatography and identified by  $^1\text{H}$  NMR spectroscopy.

## 2. Experimental

### 2.1. Materials

Fumed silica (surface area =  $384\text{ m}^2\text{ g}^{-1}$ , Sigma Aldrich, USA), poly(ethylene glycol)-block-poly(propylene glycol)-poly(ethylene glycol) (P123, average molecular weight 5800, Aldrich, USA), tetraethyl orthosilicate (TEOS, Aldrich, USA) were employed as a starting material. Cetyltrimethylammonium bromide (CTMABr, Loba Chemie, India) was used as a structure directing agent, a 25 wt% aqueous solution of tetramethylammonium hydroxide (TMAOH, Loba Chemie, India), 3-glycidoxypropyl trimethoxysilane (Aldrich, USA), 1,5,7-triazabicyclo [4.4.0] dec-5-ene (TBD, Aldrich, USA) were used without further purification.

### 2.2. Synthesis of Si-MCM-41 material

The hydrothermal synthesis was carried out in autoclave according to reported procedure [16]. The molar gel composition of the synthesis gel was: 1  $\text{SiO}_2$ :0.30 TMAOH:0.25 CTMABr:125  $\text{H}_2\text{O}$ . In a typical synthesis of a Si-MCM-41 sample, 3.0 g of fumed silica was slowly added to 5.47 g of TMAOH (25 wt%) in 10.0 g of water under vigorous stirring. Subsequently, an aqueous solution of 4.55 g of CTMABr dissolved in 30.0 g of water. The remaining 72.5 g of water was added and the stirring was continued for 15 min. Finally, the synthesis gel was taken in teflon-lined auto-clave for 48 h. The materials thus obtained were filtered, washed thoroughly first with deionized water and then with acetone, and dried at 353 K. All the samples were calcined at 773 K for 8 h in the presence of air.

### 2.3. Synthesis of SBA-15 material

Mesoporous silica SBA-15 was synthesized according to the reported procedure [17,18]. In a typical synthesis, 10 g of amphiphilic triblock copolymer, poly(ethylene glycol)-block-poly(propylene glycol)-block-poly(ethylene glycol) (average molecular weight = 5800, Aldrich Co.), was dispersed in 75 ml of water and 300 ml of 2 M HCl solution while stirring. 21.25 g of tetraethyl orthosilicate (TEOS, Aldrich Co.) was added to it. The gel was continuously stirred at 313 K for 24 h, and then finally crystallized in a teflon-lined autoclave at 373 K for 48 h. After hydrothermal treatment, the solid product was filtered, washed with deionized water, acetone and dried in air at room temperature. The solid product (SBA-15) was calcined in air at 773 K for 6 h.

### 2.4. Immobilization of 1,5,7-triazabicyclo [4.4.0] dec-5-ene in MCM-41 and SBA-15 material

Siliceous SBA-15 and MCM-41 were obtained by the above procedure and the solid residual templates were removed by calcinations. In a typical procedure for immobilization of 1,5,7-

triazabicyclo [4.4.0] dec-5-ene in MCM-41 [14,19] and SBA-15 material, 3 g of vacuum dried MCM-41 and SBA-15 was allowed to react with 4.5 mmol of 3-glycidoxy propyl trimethoxy silane (Scheme 2) in dry toluene at refluxing temperature for 24 h. Then, the samples were cooled to room temperature, filtered, washed with acetone and dried. This material is designated as glycidylated MCM-41/SBA-15 (Scheme 2). After that, the glycidylated MCM-41/SBA-15 (1.0 g) was allowed to react with 2.2 mmol of 1,5,7-triazabicyclo [4.4.0] dec-5-ene (TBD) in dry toluene (15 ml) at 298 K for 10 h. The excess TBD was removed by soxhlet extraction with DCM. The sample was designated by MCM-41/SBA-15-TBD (Scheme 2) and stored under vacuum.

### 2.5. General procedure for Michael-addition of $\beta$ -nitrostyrene to malonate

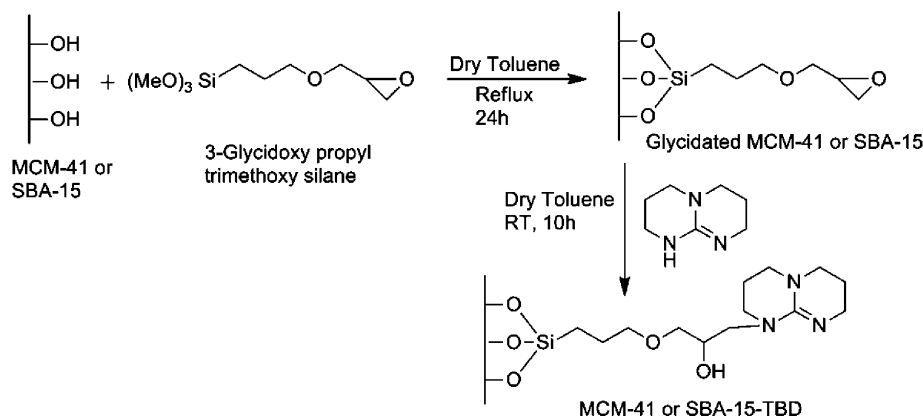
The catalytic liquid-phase reaction was performed in a two-necked round bottom flask with a water condenser under vigorously stirring in  $\text{N}_2$  atmosphere. The catalyst was preactivated at 393 K in a vacuum oven and subsequently used for the reactions under dry conditions. In a typical procedure, a mixture of  $\beta$ -nitrostyrene (10 mmol) and diethyl malonate (10 mmol) was added to a preactivated catalyst (0.2 g). The reaction mixture was stirred magnetically at 373 K for a period of 12 h. The progress of the reaction was monitored by gas chromatography (Varian model-CP-3800) equipped with capillary column and flame ionization detector (FID) as well as by thin layer chromatography (TLC). After completion of the reaction, the catalyst was separated by centrifugation. The filtrate was concentrated and corresponding product was purified through column chromatography using silica gel (100–200 mesh), petroleum ether: ethyl acetate (3:1) and confirmed through GC, GC-MS,  $^1\text{H}$  NMR,  $^{13}\text{C}$  NMR. The  $^1\text{H}$  NMR spectra were recorded in a 200 MHz using  $\text{CDCl}_3$  as solvent.

$^1\text{H}$  NMR (200 MHz,  $\text{CDCl}_3$ )  $\delta$  ppm: 1.03 (t, 3H), 1.25 (t, 3H), 3.84 (d, 1H), 4.04 (q, 2H), 4.16–4.26 (m, 3H), 4.88–4.98 (d q, 2H), 7.20–7.31 (m, 5H).

$^{13}\text{C}$  NMR (100 MHz,  $\text{CDCl}_3$ )  $\delta$  ppm: 13.7, 13.9, 42.9, 54.9, 61.9, 62.1, 77.2, 77.6, 128.0, 128.3, 128.9, 136.2, 166.8, 167.4.

### 2.6. Characterization techniques

The powder X-ray diffractograms of as-synthesized and calcined samples were recorded on a Rigaku Miniflex diffractometer ( $\text{Cu-K}\alpha$  radiation,  $\lambda = 1.54054\text{ \AA}$ ) in  $2\theta$  range  $1.5\text{--}10^\circ$  at a scanning rate of  $1^\circ\text{ min}^{-1}$  for MCM-41, and  $1.5\text{--}60^\circ$  at a scanning rate of  $2^\circ\text{ min}^{-1}$  for MCM-41. The PXRD data for SBA-15 materials were collected on a PANalytical X'pert Pro instrument using Bragg-Brentano geometry in  $2\theta$  ranges  $0.5\text{--}5.0^\circ$  at a scanning rate of  $1^\circ\text{ min}^{-1}$  ( $\lambda = 1.5416\text{ \AA}$ ). The specific surface area ( $S_{\text{BET}}$ ) and mesoporosity were checked by  $\text{N}_2$  sorption at 77 K using NOVA 1200 Quantachrome equipment. The samples were evacuated at 573 K before  $\text{N}_2$  sorption. The surface area was calculated from linear part of BET (Brunauer-Emmet-Teller) equation and the method of Barret-Joyner-Halenda (BJH) was employed to determine the pore-size distribution (PSD). Elemental analysis for C, H and N to measure the TBD loading in the catalysts were recorded by an EA 1108 elemental analyzer (Carlo-



**Scheme 2.** Immobilization of 1,5,7-triazabicyclo [4.4.0] dec-5-ene (TBD) over MCM-41 and SBA-15 materials.

alysts were recorded by an EA 1108 elemental analyzer (Carloba instruments).

Fourier transform infrared (FTIR) spectra recorded for functional group detection in the range of 400–4000  $\text{cm}^{-1}$  on a Shimadzu FTIR 8201 PC and KBr pallet was taken as reference. The IR spectra were recorded at different temperatures and 300 scans were collected for each spectrum.

The scanning electron microscopic (SEM) images were recorded on a Philips Model XL 30 instrument. The samples were loaded on stubs and sputtered with thin gold film to prevent surface charging and also to protect from thermal damage from the electron beam, prior to scanning. The samples were dispersed on Holey carbon grids and Transmission Electron Microscopic (TEM) images were scanned on a JEOL Model 1200 EX instrument operated at an accelerating voltage of 100 kV.

The solid state MAS and CP MAS NMR spectra were recorded on a Bruker MSL 300 NMR spectrometer. The finely powdered samples were placed in 7.0 mm zirconia rotors and spun at 8 kHz. The resonance frequencies of  $^{29}\text{Si}$  and  $^{13}\text{C}$  were 59.63, and 75.47 MHz, respectively. The chemical shifts were determined using 3-(trimethylsilyl) propane-1-sulfonic acid ( $\delta=0$  ppm from TMS) and adamantane ( $\delta=28.7$  ppm from TMS) as the reference compounds for  $^{29}\text{Si}$  and  $^{13}\text{C}$ , respectively.

### 3. Result and discussion

#### 3.1. Powder X-ray diffraction

The X-ray diffraction patterns of (a) MCM-41 and (b) MCM-41-TBD materials are shown in the Fig. 1. The typical hexagonal phase ( $p6mm$ ) of MCM-41 [main (1 0 0) peak with weak (1 1 0), (2 0 0) and (2 1 0) reflections] is clearly visible in all the samples. These results indicate the reflection of highly ordered mesoporosity even after incorporation of organic functional group. However, a slight decrease in the peak intensities was observed in the case of the organo base functional group (TBD) loaded samples, which might be due to partial filling of organic group inside the mesopores.

Fig. 1 shows the XRD profiles of pure SBA-15 and organo base functionalized SBA-15 materials. All the samples showed very similar XRD patterns. The samples showed three well-resolved diffraction peaks due to (1 0 0), (1 1 0) and (2 0 0) reflection in the  $2\theta$  range of 0.5–5° that could be indexed according to a 2D hexagonal  $p6mm$  symmetry [17,18]. Organic base incorporation did not alter the long-range ordering of the mesoporous structure. Inter-planar spacing ( $d_{100}$ ) and unit cell parameter ( $a_0$ ) of various functionalized SBA-15 materials are listed in Table 1. The  $d$ -spacing ( $d_{100}$ ), estimated from the position of the low-angle peak is in the range of 9.8–10.4 nm. The unit cell parameter calculated using the equa-

tion  $a_0 = 2d_{100}/\sqrt{3}$  (Table 1) is in good agreement with the values reported by others authors [17,18].

#### 3.2. Porosity measurements

Fig. 2 shows  $\text{N}_2$  adsorption–desorption isotherm and the corresponding pore size distribution curve for the calcined SBA-15 and SBA-15-TBD samples. The nitrogen adsorption/desorption isotherms of both the samples are of type IV isotherm (Fig. 2) and exhibit a H1 hysteresis loop, which is typical of mesoporous solids [17,18]. Furthermore, the adsorption branch of each isotherm showed a sharp inflection at a relative partial pressure value of about 0.55–0.64. This is the characteristic of capillary condensation within uniform pores. The position of the inflection point indicates mesopore structure, and the sharpness of these steps indicates the uniformity of the mesopore size distribution. A good match between the points of inflection on the adsorption branch of both isotherms suggests that samples have similar pore sizes (Fig. 2). The low mesopore volume was observed in case of SBA-15-TBD because the mesopores were partially blocked by functionalized organic base (Table 1). The organic-functionalized materials show some loss of surface area and a pronounced reduction in the pore volume. The calculated ‘pore diameter’ is reduced from a value of 27.6 Å and 67.1 Å in the parent MCM-41 or SBA-15 to about 26.0 Å and 58.5 Å in the MCM-41-TBD or SBA-15-TBD catalysts, respectively.

#### 3.3. Elemental microanalyses

The results microanalyses of carbon, hydrogen and nitrogen contents of the catalysts are shown in Table 1. The nitrogen content was assigned to the loading of TBD over MCM-41/SBA-15 materials. The output amount was calculated with respect to nitrogen content.

#### 3.4. FTIR-spectroscopy

Fig. 3 represents the FTIR spectra of (a) SBA-15, (b) glycidated SBA-15 and (c) SBA-15-TBD catalysts. The FTIR spectroscopy confirms the presence of the organic groups. The peaks around 1230, 1090, 804 and 465  $\text{cm}^{-1}$  are the typical Si–O–Si band attributed to the condensed silica network present in all samples. The Si–OH vibration band at 970  $\text{cm}^{-1}$  decreases after the first grafting suggesting the successful anchoring reaction between Si–OH and 3-glycidoxypropyl trimethoxysilane. The vibrational frequency of Si–OH decreases from 970 to 952  $\text{cm}^{-1}$  by organo-functionalization of 3-glycidoxypropyl trimethoxysilane and TBD over calcined SBA-15 sample. The IR peaks at 3325  $\text{cm}^{-1}$  and 3300  $\text{cm}^{-1}$  are due to free N–H bond. In the case of TBD func-

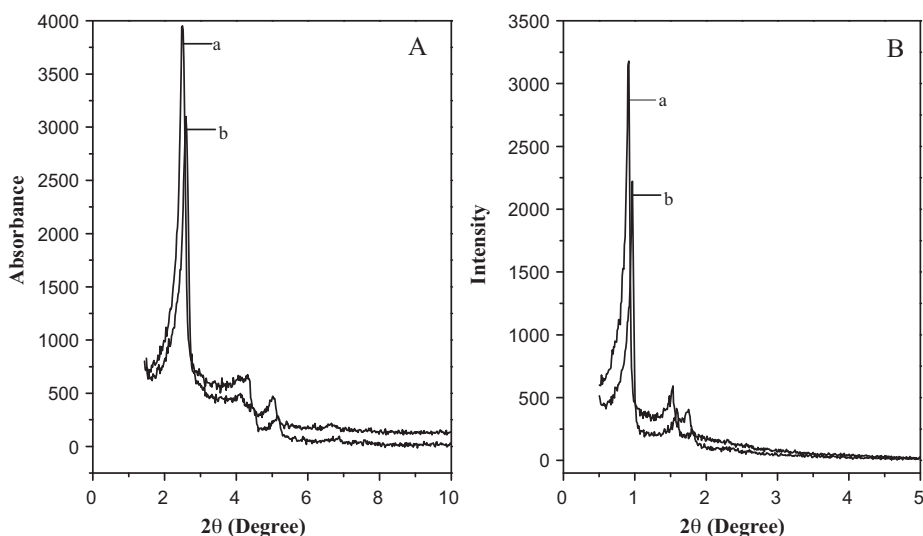


Fig. 1. Powder X-ray diffraction pattern of A: (a) MCM-41 and (b) MCM-41-TBD and B: (a) SBA-15 and (b) SBA-15-TBD catalysts.

Table 1

Physicochemical properties of MCM-41/SBA-15-TBD catalysts.

Catalysts	TBD (mmol input)	Elemental analysis			TBD (mmol output)	$S_{\text{BET}}$ ( $\text{m}^2/\text{g}$ )	$d_{100}$ ( $\text{\AA}$ )	$a_0^a$ ( $\text{\AA}$ )	Pore diameter ( $\text{\AA}$ )	Pore volume ( $\text{cm}^3/\text{g}$ )
		C	H	N						
MCM-41	–	–	–	–	–	980	37.9	43.8	27.6	1.01
MCM-41-TBD	2.2	11.9	3.3	3.9	0.92	363	37.5	43.4	26.0	0.25
SBA-15	–	–	–	–	–	733	96.6	111.7	67.1	0.95
SBA-15-TBD	2.2	16.0	3.8	4.1	0.97	391	91.6	105.9	58.5	0.52

<sup>a</sup>  $a_0$ , unit cell parameter =  $2d_{100}/\sqrt{3}$ .

tionalized SBA-15 sample, these peaks are absent indicating that TBD is attached with porous material. Characteristic peaks, due to C–H stretching vibrations of propyl spacer and cycloalkane ring, were appeared in the range of  $2863\text{--}2950\text{ cm}^{-1}$ . The spectrum c displays two new peaks at  $1541\text{ cm}^{-1}$  and  $1465\text{ cm}^{-1}$ , which are attributed to C=C and C=N bands, respectively. The peak of C–N is usually observed at  $1000\text{--}1300\text{ cm}^{-1}$ . In the  $1236\text{--}1310\text{ cm}^{-1}$  regions, the dominant contribution to the frequencies of the vibrational forms in which the different deformations of C–H bonds of methylene groups occurs are located. The stretching modes of C–C

and C–N bonds mixed with the C–H bending modes of methylene groups appear in the  $1400\text{--}1270\text{ cm}^{-1}$  range. The absorption bands in the  $1100\text{--}880$  and  $800\text{--}450\text{ cm}^{-1}$  regions are connected with stretching and deformational skeleton modes of rings and O–H deformation mode at  $1300\text{--}1400\text{ cm}^{-1}$ .

### 3.5. Scanning electron microscopy

Fig. 4 represents the scanning electron microscopy (SEM) images of calcined SBA-15 sample (A) and TBD immobilized SBA-15

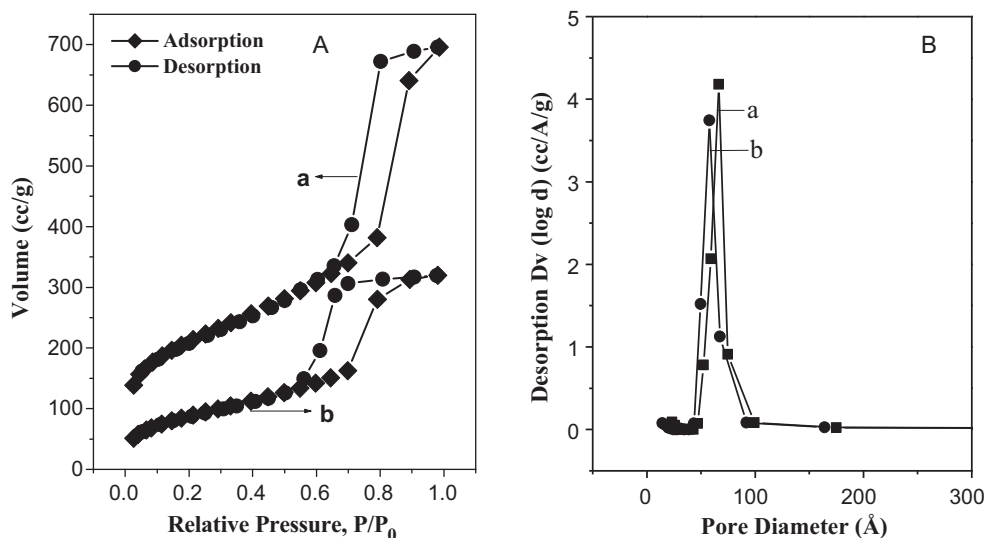
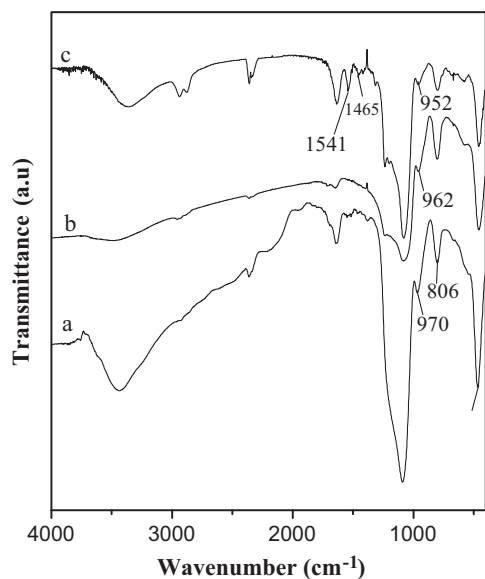
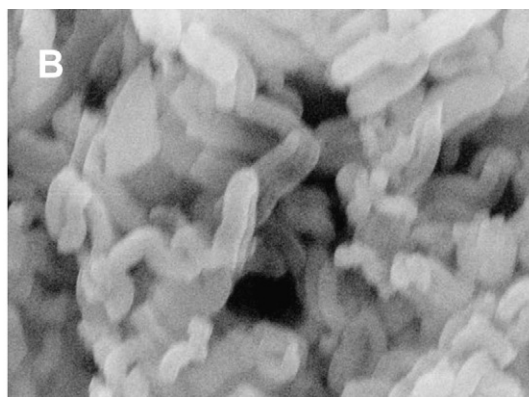
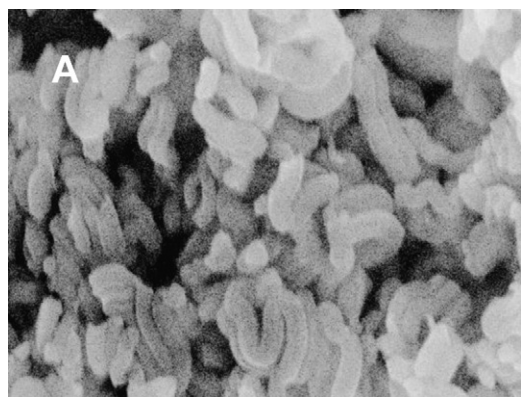


Fig. 2. (A)  $\text{N}_2$  adsorption–desorption isotherms and (B) corresponding pore size distribution curves for (a) calcined SBA-15 and (b) SBA-15-TBD catalysts.



**Fig. 3.** FTIR spectra of (a) SBA-15, (b) glycidated SBA-15 and (c) SBA-15-TBD catalysts.

sample (B). It consists of many rope-like domains with relatively uniform sizes, which are aggregated into grain-like macrostructures [18,22,23]. After organofunctionalization by TBD, SBA-15 shows a similar particle morphology, which reflects the stability of the macroscopic structure.



**Fig. 4.** SEM micrographs of (A) calcined SBA-15, and (B) SBA-15-TBD catalysts.

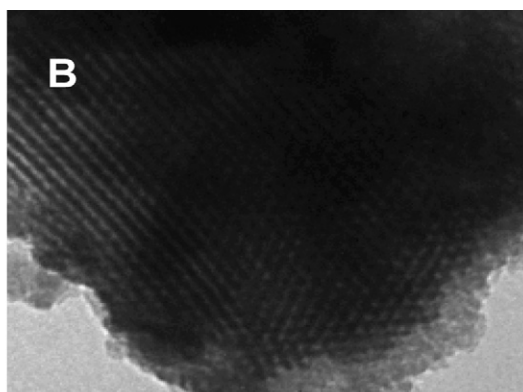
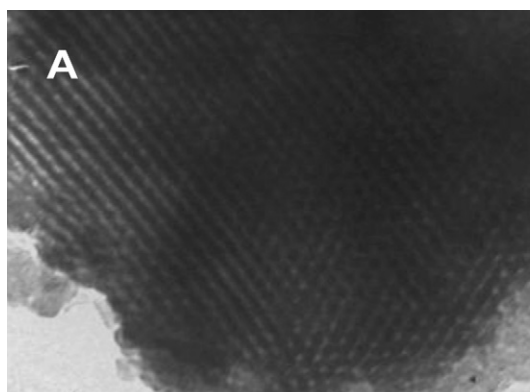


**Fig. 5.** TEM micrographs of (A) calcined SBA-15, and (B) SBA-15-TBD catalysts.

### 3.6. Transmission electron microscopy

Transmission electron microscopy (TEM) images of calcined (A) SBA-15 and (B) SBA-15-TBD samples show well-ordered hexagonal arrays of mesopores with 2D  $p6mm$  hexagonal structure (Fig. 5). The ordered mesoporous structure of the SBA-15 was slightly affected by functionalization of TBD over calcined SBA-15 sample [15,17–18,20–23].

### 3.7. Solid state $^{29}\text{Si}$ CP MAS NMR spectrum

Fig. 6 shows the  $^{29}\text{Si}$  MAS NMR spectrum of the SBA-15-TBD. It was observed from NMR spectrum that the strong resonances at  $\delta \approx -102$  and  $-110$  ppm are due to the presence of  $Q^3$  [ $(\text{SiO})_3\text{Si-OH}$ ] and  $Q^4$  [ $(\text{SiO})_3\text{Si-O-Si}$ ] species, respectively, present in the silicate framework of SBA-15-TBD materials. The presence of close-packed conformation of organic group is also manifested from the spectrum of the SBA-15-TBD sample. The two additional signals at  $\delta \approx -59$  and  $-68$  ppm are assigned to terminal ( $T^2$ ) and cross-linked ( $T^3$ ) siloxane groups, respectively, attached with pendant organic groups. These results suggest that the co-condensation process, the organic functional groups are anchored to the surface walls.

### 3.8. Solid-state $^{13}\text{C}$ CP MAS NMR spectrum

The  $^{13}\text{C}$  CP MAS NMR spectrum of SBA-15-TBD catalyst is shown in Fig. 7. The three distinct  $^{13}\text{C}$  signals observed at  $\delta \approx 9$ , 22 and 41 ppm, were assigned to  $C_1$ ,  $C_2$  and  $C_3$  atoms, respectively, of the propyl chain attached with SBA-network (Scheme 2). The characteristic peaks in the cycloalkane viz.  $C=N$  ( $\delta = 158$  ppm ( $C_{10}$ )),

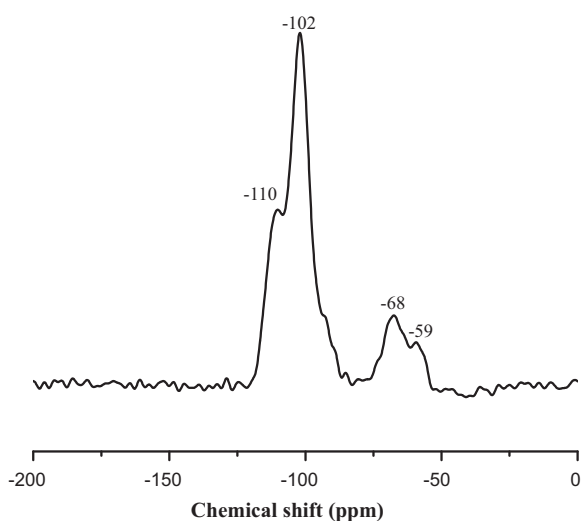


Fig. 6.  $^{29}\text{Si}$  CP MAS NMR spectrum of SBA-15-TBD catalyst.

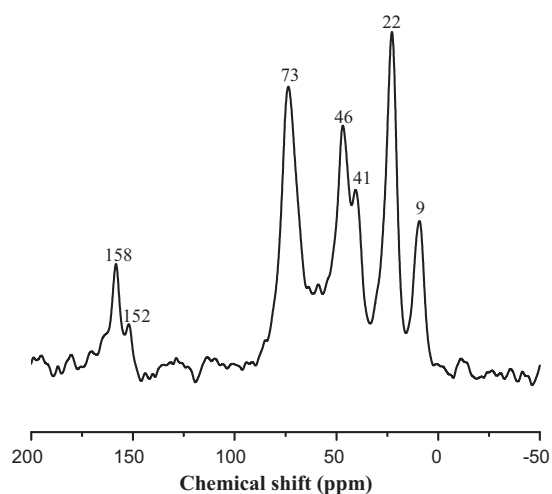


Fig. 7.  $^{13}\text{C}$  CP MAS NMR spectrum of SBA-15-TBD catalyst.

C–N bond ( $\delta = 73$  ppm,  $\text{C}_6$ ,  $\text{C}_4$ ),  $\delta = 46$  ppm ( $\text{C}_7$ ,  $\text{C}_9$ )) and C–C bond ( $\delta = 22$  ppm ( $\text{C}_8$ )) were also observed (Fig. 7).

### 3.9. Catalytic activities

#### 3.9.1. Effect of reaction time

Fig. 8 A shows the effect of reaction time on conversion of  $\beta$ -nitrostyrene over MCM-41-TBD and SBA-15-TBD catalyst in Michael-addition of  $\beta$ -nitrostyrene with diethyl malonate (Scheme 1) to produce corresponding diethyl 2-(2-nitro-1-phenylethyl) malonate. Ethanol (EtOH) was used as a solvent in these experiments at 353 K. Although, each experiment was continued for ca. 12 h, there was only marginal increase in the conversion after 9 h of the reaction. The individual experiments were performed for MCM-41-TBD and SBA-15-TBD catalyst under  $\text{N}_2$  atmosphere. It was observed that the conversion of  $\beta$ -nitrostyrene was reached 65 and 71% within 9 h over the MCM-41-TBD and SBA-15-TBD catalyst, respectively (Fig. 8 A).

The catalytic activity was also examined for Michael-addition of  $\beta$ -nitrostyrene and diethyl malonate over (a) MCM-41-TBD and (b) SBA-15-TBD catalyst under solvent free system at 353 K. The reaction data are plotted as function of time in Fig. 8B. Under solvent free system, 67 and 75% conversion of  $\beta$ -nitrostyrene were obtained within 9 h over the MCM-41-TBD and SBA-15-TBD catalyst, respectively (Fig. 8B). The selectivity towards the product over both catalysts was found to be 100%. It was observed that there was marginal increase in the conversion of  $\beta$ -nitrostyrene under solvent free condition (vis-à-vis in the presence of solvent, ethanol) over the MCM-41-TBD and SBA-15-TBD catalyst (Table 2). It was observed that SBA-15-TBD catalyst exhibited higher activity compared to that of MCM-41-TBD under same reaction (Table 1) and this is because of the larger pore size of SBA-51 materials. Therefore, for further studies were carried out using SBA-15-TBD catalyst.

#### 3.9.2. Effect of catalyst amount

To optimize the amount of catalyst for the Michael-addition of  $\beta$ -nitrostyrene with diethyl malonate (Scheme 1), the reaction was carried out under solvent free condition over SBA-15-TBD catalyst for 12 h using varying amount of catalyst (3.5–13.3 wt% with respect to  $\beta$ -nitrostyrene). The conversion of  $\beta$ -nitrostyrene was found to increase from 35 to 81% when catalyst amount was increased from 0.05 (3.3 wt%) to 0.2 g (13.3 wt%) (Fig. 9 curves a–d).

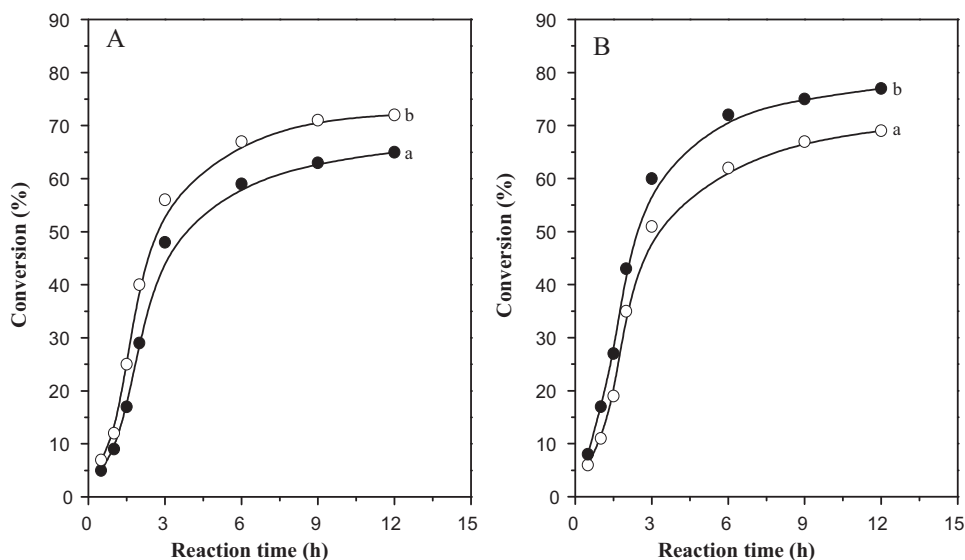


Fig. 8. Effect of reaction time on conversion for Michael-addition of  $\beta$ -nitrostyrene and diethyl malonate over (a) MCM-41-TBD and (b) SBA-15-TBD catalyst with (A) ethanol as solvent at 353 K and (B) no solvent at 353 K.

**Table 2**

Michael-addition of  $\beta$ -nitrostyrene with diethyl malonate over MCM-41-TBD and SBA-15-TBD catalyst at different temperature<sup>a</sup>.

Catalysts	Solvent	Temperature (K)	Conv. <sup>b</sup> (mol%)	TON <sup>c</sup>
MCM-41-TBD	Ethanol	353	63	33.9
MCM-41-TBD	No solvent	353	67	36.0
SBA-15-TBD	Ethanol	353	71	36.3
SBA-15-TBD	No solvent	353	75	38.4
SBA-15-TBD	No solvent	373	81	41.4
SBA-15-TBD	No solvent	333	50	25.6
SBA-15-TBD	No solvent	298	23	11.7

<sup>a</sup> Reaction condition:  $\beta$ -nitrostyrene (10 mmol), malonate (10 mmol), reaction time 9 h, catalyst amount = 0.2 g.

<sup>b</sup> Conversion (Conv.) with respect to  $\beta$ -nitrostyrene and based on GC analysis.

<sup>c</sup> TON is given as moles of  $\beta$ -nitrostyrene transformed per mole of nitrogen.

The product selectivity was always obtained ca. 100%. It is reasonable to assume that the interaction of the reactant molecules with the active sites of the SBA-15-TBD catalyst is commensurate with increase in the amount of catalyst in the reaction mixture and hence the availability of a higher number of active sites. However, the reaction showed only marginal increase in the conversion from 76 to 81% with further increasing the catalyst amount from 0.15 to 0.20 g (curves c and d). Hence, about 10 wt% catalysts is required amount for significant Michael-addition of  $\beta$ -nitrostyrene with diethyl malonate.

### 3.9.3. Effect of temperature

The effect of temperature was examined for Michael-addition of  $\beta$ -nitrostyrene with diethyl malonate under solvent free condition over the SBA-15-TBD catalyst for 12 h (Fig. 10). Individual experiments were performed at each temperature under identical reaction conditions. The progress of the reaction was monitored by gas chromatography. The rate of  $\beta$ -nitrostyrene conversion was increased from 23 to 81% with increasing temperature from 298 to 373 K as expected (curves a–d). This indicates that the catalyst is quite stable and the reaction was free from the diffusion limitation at higher temperatures. Furthermore, the increased con-

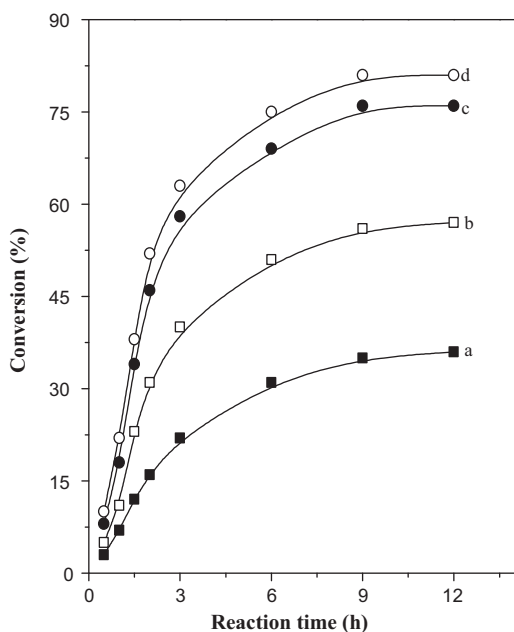


**Fig. 9.** Plot of conversion vs reaction time for Michael-addition of  $\beta$ -nitrostyrene with diethyl malonate using different amount of SBA-15-TBD catalyst under solvent free condition at 373 K. Curves (a) 0.05 g (3.3 wt%), (b) 0.1 g (6.6 wt%), (c) 0.15 g (10 wt%) and (d) 0.2 g (13.3 wt%).

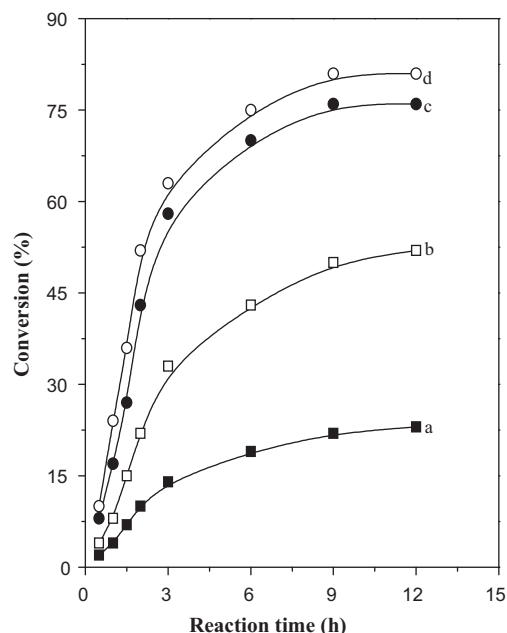


**Fig. 10.** Plot of conversion vs reaction time for Michael-addition of  $\beta$ -nitrostyrene with diethyl malonate over SBA-15-TBD catalyst at different temperature. Curves (a) 298 K, (b) 333 K, (c) 353 K and (d) 373 K.

version at higher temperatures clearly shows that this reaction demands high-activation energy. It is also evident that the active sites are activated more at higher temperatures, which leads to a higher rate of attack of nucleophile (malonate) to electrophile (nitrostyrene). Consequently, the conversion of  $\beta$ -nitrostyrene increases with an increase in the reaction temperature from 298 to 373 K (Fig. 10 curves a–d). Again, the product selectivity was found almost  $\sim$ 100% in each case.

### 3.9.4. Recycle studies

In order to check the recyclability and stability of the catalyst, the Michael-addition of  $\beta$ -nitrostyrene with diethyl malonate was carried out for three consecutive reaction cycles using SBA-15-TBD catalyst. After the reaction, the catalyst was filtered from hot reaction mixture, washed with dichloromethane and used for three successive times without any further activation. The reactants were taken with respect to the amount of the catalyst recovered after each reaction cycle. All reactions were carried out under solvent-free condition at 373 K for 9 h. The conversion and turn over number (TON) obtained for the period of recycle studies of the SBA-15-TBD catalyst are given in Table 3. The conversion was decreased from 81 to 76% in the first recycle, and then it decreases slowly upto 69% (3rd recycle) as shown in Table 3. The conversion decreased due to loss of nitrogen content (due to leaching) in the solid catalyst as confirmed by elemental analysis (Table 3). Nevertheless, the TON

**Table 3**

Recycle studies of SBA-15-TBD catalyst for Michael-addition of  $\beta$ -nitrostyrene and diethyl malonate under solvent free condition.

Recycle no.	Elemental analysis (wt%)			Conv. <sup>a</sup> (mol%)	TON <sup>b</sup>	Selectivity (%)
	C	H	N			
Fresh	16.0	3.8	4.1	81	41.4	100
1st	15.4	3.6	3.9	77	41.0	100
2nd	14.3	3.1	3.6	71	41.1	100
3rd	11.9	2.8	3.2	69	41.5	100

<sup>a</sup> Conversion (Conv.) with respect to  $\beta$ -nitrostyrene and based on GC analysis.

<sup>b</sup> TON is given as moles of  $\beta$ -nitrostyrene transformed per mole of nitrogen.

**Table 4**  
Michael-addition of  $\beta$ -nitrostyrene with different malonate over SBA-15-TBD catalyst<sup>a</sup>.

Entry	Malonate	Conv. <sup>c</sup> (mol%)	Product
1.	Diethyl malonate	81	
2.	Dimethyl malonate	84	
3.	Dimethyl methylmalonate	86	
4.	Dimethyl methoxymalonate	89	
5.	Diethyl ethylmalonate	65	
6. <sup>b</sup>	Diethyl phenylmalonate	0	

<sup>a</sup> Reaction condition:  $\beta$ -nitrostyrene (10 mmol), malonate (10 mmol), no solvent, reaction temperature 373 K, reaction time 9 h, catalyst amount = 0.2 g.

<sup>b</sup> Reaction time 24 h.

<sup>c</sup> Conversion (Conv.) with respect to  $\beta$ -nitrostyrene and based on GC analysis.

was found to remain unchanged when calculated on the basis of the N remaining in the solid catalysts after these consecutive test runs.

### 3.9.5. Michael-addition of $\beta$ -nitrostyrene with different malonates

The different substrates were examined for the Michael-addition of  $\beta$ -nitrostyrene with different malonates over SBA-15-TBD catalyst. All the reactions were performed under solvent free condition at 373 K for 9 h in  $N_2$  atmosphere. The corresponding results are summarized in Table 4. The product selectivity of all the reactions was observed ca. 100%. As compared to dimethyl malonate (Entry 2), less conversion was obtained when diethyl malonate was used (Entry 1). This is because of the less electron delocalization in diethyl malonate (Entry 1) and due to the more electron donating nature of ethoxy group in it, which results in the less electronegative  $\alpha$ -substituted malonate. Hence, the attack of nucleophile to electrophile will be less facile in diethyl malonate than dimethyl malonate. Slightly less conversion was obtained in the case of dimethyl methylmalonate (Entry 3) than dimethyl methoxymalonate (Entry 4). This is mainly because of the more electron-donating group ( $-OMe$  group) present in dimethyl methoxymalonate (Entry 4). Since, methoxy group ( $-OMe$ ) is more electron-donating than methyl group, so, the formation of nucleophile in  $\alpha$ -substituted malonate will be more in dimethyl methoxymalonate (Entry 4) than dimethyl methylmalonate (Entry 3). In the case of Entry 5, the significantly low conversion was obtained for the reaction of  $\beta$ -nitrostyrene and diethyl ethylmalonate. However, no conversion was observed for the reaction

**Table 5**  
Michael-addition of different nitrostyrene with different malonate over SBA-15-TBD catalyst<sup>a</sup>.

Entry	Malonate	Nitrostyrene	Conv. <sup>b</sup> (mol%)	Product
1.	Diethyl malonate	p-OMe-NO <sub>2</sub> Styrene	79	
2.	Diethyl malonate	p-Cl-NO <sub>2</sub> Styrene	84	
3.	Dimethyl malonate	p-OMe-NO <sub>2</sub> Styrene	84	
4.	Dimethyl malonate	p-Cl-NO <sub>2</sub> Styrene	91	

<sup>a</sup> Reaction condition: nitrostyrene (10 mmol), malonate (10 mmol), no solvent, reaction temperature 373 K, reaction time 9 h, catalyst amount = 0.2 g.

<sup>b</sup> Conversion (Conv.) with respect to  $\beta$ -nitrostyrene and based on GC analysis.

of  $\beta$ -nitrostyrene with diethyl phenylmalonate (Entry 6, 0%) even after the reaction was carried out for 24 h. This is mainly because of the presence of more sterically hindered phenyl group in  $\alpha$ -substituted malonate (Entry 6). Hence, it is not possible to make nucleophilic center in  $\alpha$ -substituted malonate. Therefore, attack of nucleophile to electrophile did not occur in this reaction.

### 3.9.6. Michael-addition of different nitrostyrenes with different malonates

The Michael-addition was also carried out with different nitrostyrenes and different malonates under identical reaction condition and these results are summarized in Table 5. The conversion obtained was 79% and 84% for the reactions of diethyl malonate with p-OMe-NO<sub>2</sub> styrene (Entry 1) and p-Cl-NO<sub>2</sub> styrene (Entry 2), respectively. Similarly, the reaction of dimethyl malonate with p-OMe-NO<sub>2</sub> styrene (Entry 3) and p-Cl-NO<sub>2</sub> styrene (Entry 4) gave conversion of 84 and 91%, respectively. High conversion was observed when the reaction was carried out with p-Cl-NO<sub>2</sub> styrene (Entry 2, 4) and diethyl malonate as well as with dimethyl malonate. This is mainly because of the presence of electron-withdrawing group ( $-Cl$ ) in the 4-position of nitrostyrene (Entry 2 and 4). Since, chlorine has more electron-withdrawing power than methoxy ( $-OMe$ ) group, so, the electropositive character will be high at  $\beta$ -carbon in nitro styrene. Hence, attack of nucleophile to electrophile will be more facile which leads to the more conversion of the reaction.

## 4. Conclusions

To conclude, a well-organized and environmentally friendly catalyst has been successfully synthesized by a facile two-step route immobilization and a methodology has been developed for

carbon–carbon bond formation reaction such as Michael-addition of  $\beta$ -nitrostyrene to malonate. This methodology is applicable to wide range of substrates making it a useful addition reaction for the organic chemists. Since, 1,5,7-triazabicyclo [4.4.0] dec-5-ene (TBD) is inexpensive and commercially available, so converting homogeneous TBD into heterogeneous TBD catalyst is a better option as it can be easily filtered as well as can be recycled for several times. The loss of activity is observed to some extent after three recycles, which may be because of the decrease of nitrogen content and loss of crystallinity of the SBA-15-TBD catalyst.

### Acknowledgements

The authors are grateful to Dr. Selvaraj, Ms. S. Violet and Mr. R.K. Jha, for their kind cooperation with XRD, surface area analysis, respectively. PK thanks CSIR, New Delhi, India, for grant of research fellowship.

### References

- [1] (a) D.H.R. Barton, J.D. Elliott, S.D. Géro, *J. Chem. Soc. Perkin Trans. 1* (1982) 2085–2090;  
(b) F.P. Schmidtchen, *Chem. Ber.* 113 (1980) 2175–2182.
- [2] (a) B. Kovačević, Z.B. Maksić, *Org. Lett.* 3 (2001) 1523–1526;  
(b) I. Kaljurand, T. Rodima, A. Pihl, V. Maemets, I. Leito, I.A. Koppel, M. Mishima, *J. Org. Chem.* 68 (2003) 9988–9993.
- [3] (a) D. Simoni, M. Rossi, R. Rondanin, A. Mazzali, R. Baruchello, C. Malagutti, M. Roberti, F.P. Invidata, *Org. Lett.* 2 (2000) 3765–3768;  
(b) M.G. Edwards, J.M.J. Williams, *Angew. Chem. Int. Ed.* 41 (2002) 4740–4743.
- [4] D. Simoni, R. Rondanin, M. Morini, R. Baruchello, F.P. Invidata, *Tetrahedron Lett.* 41 (2000) 1607–1610.
- [5] A. Horváth, *Tetrahedron Lett.* 37 (1996) 4423–4426.
- [6] V.K. Aggarwal, A. Mereu, *Chem. Commun.* (1999) 2311–2312.
- [7] M. Watanabe, A. Ikagawa, H. Wang, K. Murata, T. Ikariya, *J. Am. Chem. Soc.* 126 (2004) 11148–11149.
- [8] (a) J. Ji, D.M. Barnes, J. Zhang, S.A. King, S.J. Wittenberger, H.E. Morton, *J. Am. Chem. Soc.* 121 (1999) 10215–10216;  
(b) D.M. Barnes, J. Ji, M.G. Fickes, M.A. Fitzgerald, S.A. King, H.E. Morton, F.A. Plagge, M. Preskill, S.H. Wagaw, S.J. Wittenberger, J. Zhang, *J. Am. Chem. Soc.* 124 (2002) 13097–13105;  
(c) J. Wang, H. Li, W. Duan, L. Zu, W. Wang, *Org. Lett.* 7 (2005) 4713–4716.
- [9] (a) N. Mase, K. Watanabe, H. Yoda, K. Takabe, F. Tanaka, C.F. Barbas, *J. Am. Chem. Soc.* 128 (2006) 4966–4967;  
(b) S.H. McCooney, S.J. Connon, *Org. Lett.* 9 (2007) 599–602.
- [10] L. Zu, J. Wang, H. Li, W. Wang, *Org. Lett.* 8 (2006) 3077–3079.
- [11] J. Wang, H. Li, L. Zu, W. Wang, *Org. Lett.* 8 (2006) 1391–1394.
- [12] (a) Y.-X. Jia, S.-F. Zhu, Y. Yang, Q.-L. Zhou, *J. Org. Chem.* 71 (2006) 75–80;  
(b) S.-F. Lu, D.-M. Du, J. Xu, *Org. Lett.* 8 (2006) 2115–2118;  
(c) C. Lin, J. Hsu, M.N.V. Sastry, H. Fang, Z. Tu, J.-T. Liu, Y. C-Fa, *Tetrahedron* 61 (2005) 11751–11757.
- [13] L. Soldi, W. Ferstl, S. Loebbecke, R. Maggi, C. Malmassari, G. Sartori, S. Yada, *J. Catal.* 258 (2008) 289–295.
- [14] Y.V.S. Rao, D.E. De Vos, P.A. Jacobs, *Angew. Chem. Int. Ed.* 36 (1997) 2661–2663.
- [15] R. Srivastava, *J. Mol. Catal. A: Gen.* 264 (2007) 146–152.
- [16] (a) C.T. Kresge, M.E. Leonowicz, W.J. Roth, J.C. Vartuli, J.S. Beck, *Nature* 359 (1992) 710–712;  
(b) J.S. Beck, J.C. Vartuli, W.J. Roth, M.E. Leonowicz, C.T. Kresge, K.D. Schmitt, C.T.-W. Chu, D.H. Olson, E.W. Sheppard, S.B. McCullen, J.B. Higgins, J.L. Schlenker, *J. Am. Chem. Soc.* 114 (1992) 10834–10843.
- [17] D. Zhao, J. Feng, Q. Huo, N. Melosh, G.H. Fredrickson, B.F. Chmelka, G.D. Stucky, *Science* 279 (1998) 548–552.
- [18] D. Zhao, Q. Huo, J. Feng, B.F. Chmelka, G.D. Stucky, *J. Am. Chem. Soc.* 120 (1998) 6024–6036.
- [19] D.E. De Vos, M. Dams, B.F. Sels, P.A. Jacobs, *Chem. Rev.* 102 (2002) 3615–3640.
- [20] R. Srivastava, D. Srinivas, P. Ratnasamy, *J. Catal.* 233 (2005) 1–15.
- [21] R. Srivastava, D. Srinivas, P. Ratnasamy, *Microporous Mesoporous Mater.* 90 (2006) 314–326.
- [22] D.P. Sawant, A. Vinu, N.E. Jacob, F. Lefebvre, S.B. Halligudi, *J. Catal.* 235 (2005) 341–352.
- [23] R.I. Kureshy, I. Ahmad, N.H. Khan, S.H.R. Abdi, K. Pathak, R.V. Jasra, *J. Catal.* 238 (2006) 134–141.